Affine Invariance Contour Descriptor Based on the Equal Area Normalization

Yang Mingqiang, Kpalma Kidiyo, Ronsin Joseph

Abstract— In this study, we present a one dimensional descriptor for the two dimensional object silhouettes which in theory remains absolutely invariant under affine transforms. The proposed descriptor operates on the affine enclosed area. We design a normalizing contour method. After this normalization, the number of points on a contour between two appointed positions doesn't change with affine transforms. We prove that for the filtered contour, the area of a triangle whose vertices are the centroid of the contour and a pair of successive points on the normalized contour is linear under affine transforms. Experimental results indicate that the proposed method is invariant to: boundary starting point variation, affine transforms even in the case of high deformations and noise on shapes in a given. We also propose a method to simulate the noise contaminating the test shapes and define the signal-to-noise ratio for a shape. In addition, the proposed normalization method can be associated to other algorithms for increasing their robustness to affine transforms and decreasing their complexity in similarity measurements.

Index Terms—Affine-invariant, Contour, Descriptor, Filter, Noise.

Ⅰ. INTRODUCTION

The advent of multimedia and large image collections in different domains and applications bring a necessity for image retrieval systems. These systems are supposed to retrieve images in an effective manner based on a user's input query. Image retrieval is based on observation of an ordering of match scores obtained by searching through a database. The key challenges in building a retrieval system are the choice of attributes, their representations, query specification methods, match metrics and indexing strategies.

Considerable amount of information exists in two dimensional boundaries of objects which enable us to recognize objects without using further information. A shape is originally defined by x and y coordinates of its boundary points which are subject to changes if the camera is allowed to change its viewpoint with respect to the object, the resulting boundary of the object will be deformed. This deformation can be approximated by general affine transforms. As a result, a shape representation must be robust under similarity transformation which includes scaling, changes in orientation, shearing and translation. A number of shape representations have been suggested to recognize shapes even under affine transforms. Some of them are the extensions of well-known methods such as dyadic wavelet transform [1], Fourier descriptors [2], affine curvature scale space (CSS) [3], affine arc length [4] and moment invariants [5], etc. In these methods, the basic idea is to use a parameterization which is robust with respect to affine transforms.

Yang Mingqiang is with the IETR-INSA, UMR-CNRS 6164, Rennes, 35043, France. (Phone: +33 233 23 23 86 15; Fax: +33 233 23 82 62; E-mail: myang@ens.insa-rennes.fr)
Kpalma Kidiyo is with the IETR-INSA, Rennes, 35043, France.
Ronsin Joseph is with the IETR-INSA, Rennes, 35043, France.

In this paper, to extract an affine invariant attribute, a new algorithm based on area equal normalization is proposed. In theory this attribute is absolutely robust under the affine transforms, even with serious transformations. Experimental results show that the proposed algorithm is also rather insensitive to noise. In addition, a high computationally efficient object recognition scheme is briefly presented.

Ⅱ. FUNDAMENTAL CONCEPTS

A. Closed Curve

Let us consider the discrete parametric equation of a closed curve:

$$\Gamma(\mu) = (x(\mu), y(\mu)) \qquad (2.1)$$

where $\mu \in \{0, \ldots, N-1\}$. In general, curves of an application may have been parameterized with different number of vertices N.

B. Affine Transforms

The affine transformed version of a shape can be represented by the following equations [6]:

$$\begin{bmatrix} x_a(\mu) \\ y_a(\mu) \end{bmatrix} = \begin{bmatrix} a & b \\ c & d \end{bmatrix} \begin{bmatrix} x(\mu) \\ y(\mu) \end{bmatrix} + \begin{bmatrix} e \\ f \end{bmatrix} = A \begin{bmatrix} x \\ y \end{bmatrix} + B \qquad (2.2)$$

Where $x_a(\mu)$ and $y_a(\mu)$ represent the coordinates of the transformed shape. Translation is represented by matrix B, while scaling, rotation and shear are reflected in the matrix A. They are represented by the following matrices:

$$A_{Scaling} = \begin{bmatrix} S_x & 0 \\ 0 & S_y \end{bmatrix}, A_{Rotation} = \begin{bmatrix} \cos\theta & -\sin\theta \\ \sin\theta & \cos\theta \end{bmatrix}, A_{Shear} = \begin{bmatrix} 1 & k \\ 0 & 1 \end{bmatrix}$$

If S_x is equal to S_y, $A_{Scaling}$ represents a uniform scaling. A shape is not deformed under rotation, uniform scaling and translation. However, non-uniform scaling and shear contribute to the shape deformation under general affine transforms.

C. Affine Invariant Parameters

There are two parameters which are linear under affine transforms. They are the *affine arc length*, and the *enclosed area*.

The first parameter can be derived based on the properties of determinants. It is defined as follows:

$$\tau = \int_a^b [x'(\mu)y''(\mu) - x''(\mu)y'(\mu)]^{1/3} d\mu \qquad (2.3)$$

The second affine invariant parameter is enclosed area which is derived based on the property of affine transforms: Under an affine mapping, all areas are changed in the same ratio. Based on this property, Arbter et al. [2] defined a parameter σ, which is linear under a general affine transform, as follows:

$$\sigma = \frac{1}{2} \int_a^b |x(\mu)y'(\mu) - y(\mu)x'(\mu)| d\mu \qquad (2.4)$$

where $x(\mu)$ and $y(\mu)$ are the coordinates of points on the

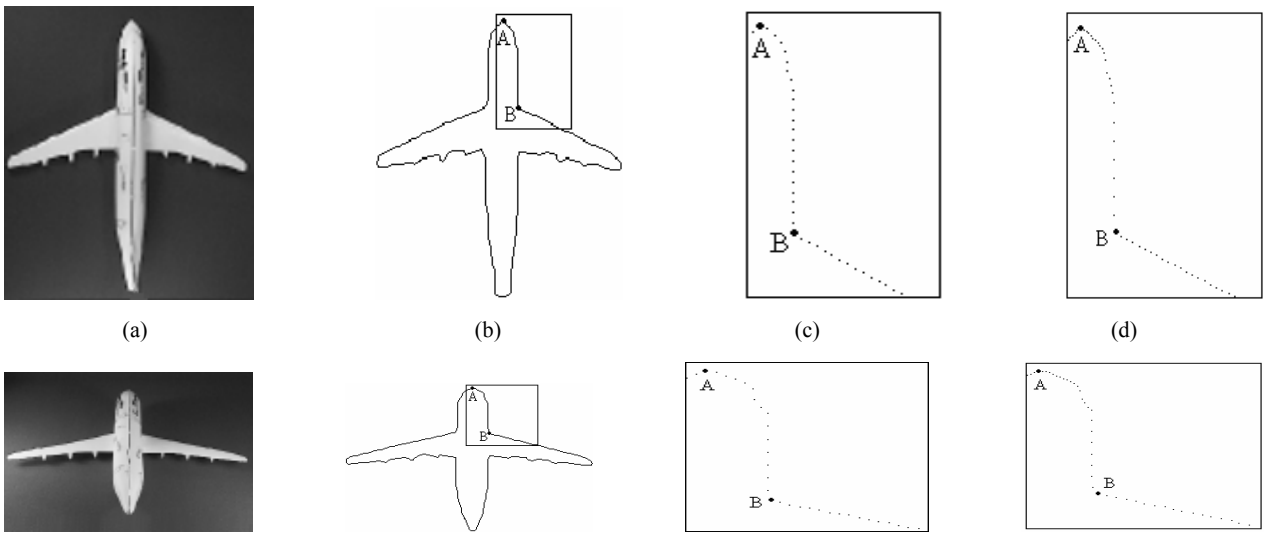

Fig.1. The comparison of equidistant vertices normalization and equal area normalization. (a) is the image of top viewpoint of a plane. (b) is the contour of image (a). (c) is a part of contour (b) normalized by equidistant vertices. (d) is a part of contour (b) normalized by equal area. (e) is the image of back top viewpoint of the plane. (f) is the contour of image (e). (g) is a part of contour (f) normalized by equidistant vertices. (h) is a part of contour (f) normalized by equal area.

contour with the origin of system located at the centroid of the contour. The parameter σ is essentially the cumulative sum of triangular areas produced from connecting the centroid to a pairs of successive vertices on the contour.

III. EQUAL AREA NORMALIZATION

All points on a shape contour could be expressed in terms of the parameter of index points along the contour curve from a specified starting point. With the affine transforms, the position of each point changes and it is possible that the number of points between two specified points changes too. So if we parameterize the contour using the equidistant vertices, the index point along the contour curve will change under affine transforms. For example, Fig.1(a) is the top viewpoint of a plane, and (e) is the back top viewpoint of the plane, so (e) is one of affine transforms of the image (a). Via region segmentation or edge following, we get the contours of the images (b) and (f). (c) and (g) are the parts of the contour (b) and (f) normalized by equal distance respectively. In Fig.1(c), the number of points between the appointed points A and B is 21; however, the number is 14 in Fig1.(g). So the contour normalised by equidistant vertices is variance to possible affine transforms.

In order to be invariance under affine transforms, a novel curve normalization approach is proposed that provides an affine invariant description of object curves at a low computational cost, while at the same time preserving all information on curve shapes. This approach is equal area normalization (EAN) and we present it as follow:

All points on a shape contour could be expressed in terms of two periodic functions $C(\mu') = (x(\mu'), y(\mu'))$, where variable μ' is measured along the contour curve from a specified starting point.

1) Normalize the contour to N points with equidistance vertices. The new periodic functions are $C(\mu) = (x(\mu), y(\mu))$ and all the points on the contour are p_μ .where $\mu \in [0, N-1]$.

2) Calculate the second-order moments of the contour as its centroid G.

3) Transfer the contour to make centroid G to be at the origin of coordinates.

4) The last point $(x(N), y(N))$ is assumed to be the same as the first. Compute the area of the contour using the formula:

$$S = \frac{1}{2}\sum_{\mu=0}^{N-1} \left| \; x(\mu)y(\mu+1) - x(\mu+1)y(\mu) \; \right| \qquad (3.1)$$

where $\frac{1}{2}\left|x(\mu)y(\mu+1) - x(\mu+1)y(\mu)\right|$ is the area of the triangle whose vertices are p_μ *(x(μ), y(μ)),* $p_{\mu+1}$ *(x(μ+1), y(μ+1))* and centroid G (cf. Fig.2).

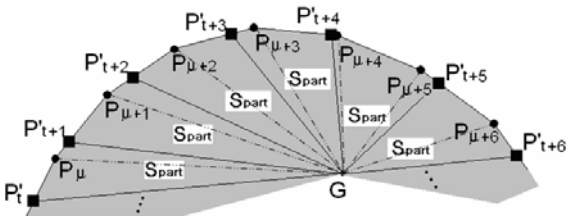

Fig.2. The method of normalization equal area. "●"is the vertex p of equidistant vertices normalization, and "■" is the point p' of equal area normalization. G is the centroid of the contour.

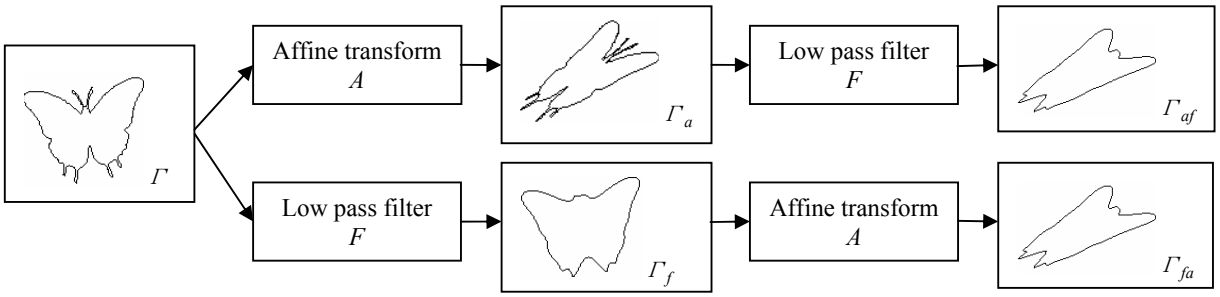

Fig.3. Demonstration of the theorem1

5) Let the number of points on the contour after EAN be N too. Of course, any other number of points could be chosen. Therefore, after EAN, each enclosed area S_{part} defined by the two successive points on the contour and centroid equal to $S_{part} = S / N$.

Suppose all the points on the contour after EAN are p'_t. Let $C(t) = (x'(t), y'(t))$ represent the contour, where $t \in [0, N-1]$. Choose the starting point p_0 $(x(0), y(0))$ on the equidistant vertices normalization as the starting point p_0' $(x'(0), y'(0))$ of the EAN, on the segment $p_0 p_1$, we seek for a point $p_1'(x'(1), y'(1))$, let thearea $s(0)$ of the triangle whose vertices are p_0' $(x'(0), y'(0))$, $G(0)$ and $p_1'(x'(1), y'(1))$ equal to S_{part}. If there is not point to satisfy the condition, then we seek for the point p_1' on the segment $p_1 p_2$. So the area $s(0)$, which is the sum of the areas of triangle $p_0 G p_1$ and triangle $p_1 G p_1'$, equal to S_{part}. If there is not the point to satisfy the condition yet, we continue to seek for this point at the next segment until the condition is satisfied. This point p_1' is the second point on the normalized contour.

6) From point $p_1'(x'(1), y'(1))$, we use the same method to calculate all the points $p_t'(x'(t), y'(t))$, $t \in [0, N-1]$ along the contour. Because the area of each closed zone, for example, the polygon $p'_t [p_\mu p_{\mu+1} \cdots] p'_{t+1} G$ $t \in [0, N-2]$ equal to S_{part}, the total area of $N-1$ polygon is $(N-1) \cdot S_{part}$. According to 5), we know it equal to $S - S_{part}$. So the area of the last zone $p_{N-1}' G p_0'$ equal to S_{part} exactly.

From Fig.2 we know, the area of the triangle $p'_t G p'_{t+1}$ equal to the area S_t of polygon $p'_t [p_\mu p_{\mu+1} \cdots] p'_{t+1} G$ approximately if the distance between the two points $p_\mu p_{\mu+1}$ is close enough or the number N of the points on the contour is big enough. Therefore, we can use the points p'_t $t \in [0, N-1]$ to replace the points p_μ $\mu \in [0, N-1]$. Then the process of EAN is accomplished.

According to subsection Ⅱ.C, after this normalization, the number of vertices between the two appointed points on a contour is invariant under affine transforms. Fig.1(d) and (h) are the same parts of Fig.1(c) and (g) respectively. We notice that the distance between the consecutive points is not uniform. In Fig.1(d), the number of points between the appointed points A and B is 23, the number is also 23 in Fig.1(g). Therefore, after applying EAN, the index of the points on a contour can remain stability with their positions under affine transforms. This property will be very advantageous to extract the robust attributes of a contour and decrease complexity in the similarity measure. We can also use EAN to the others algorithm, to improve their robustness with affine transforms. For example, before do the algorithm of curvature scale space (CSS), the contour is normalized by EAN, all the maximum points in the image CSS will not change under affine transforms. This is beneficial to calculate the similarity between two CSS attributes.

In the following, we will study the part area S_{part} change with the effect of affine transforms and filtering.

Ⅳ. NORMALIZED PART AREA VECTOR

In this section, we look for the existing relations between the part area S_{part}, affine transforms and low-pass filtering.

THEOREM1:

If $\Gamma_a(x_a(\mu), y_a(\mu))$ is the transformed version of a planar curve $\Gamma(x(\mu), y(\mu))$ under an affine transform A, where μ is an arbitrary parameter, $\Gamma_{af}(x_{af}(\mu), y_{af}(\mu))$ notes that Γ_a is filtered by a linear low-pass filter F; and if $\Gamma_f(x_f(\mu), y_f(\mu))$ notes that Γ is filtered by the same low-pass filter F, $\Gamma_{fa}(x_{fa}(\mu), y_{fa}(\mu))$ refers to the transformed version of Γ_f under the same affine transform A. Planar curve Γ_{af} is then the same as planar curve Γ_{fa}. In other words: $F[A(\Gamma)]=A[F(\Gamma)]$. (cf. Fig.3)

PROOF:

From Eq.2.2 we have

$$x_a(\mu) = ax(\mu) + by(\mu) + e \qquad (4.1)$$

$$y_a(\mu) = cx(\mu) + dy(\mu) + f \qquad (4.2)$$

Translation is represented by e and f. For all affine transforms contour, we transfer the centre gravity to origin. So the represents of translation e and f can be removed. Therefore, the affine transform can be represented by two simple formulae:

$$x_a(\mu) = ax(\mu) + by(\mu) \qquad (4.3)$$

$$y_a(\mu) = cx(\mu) + dy(\mu) \qquad (4.4)$$

The computation starts by convolving each coordinate of

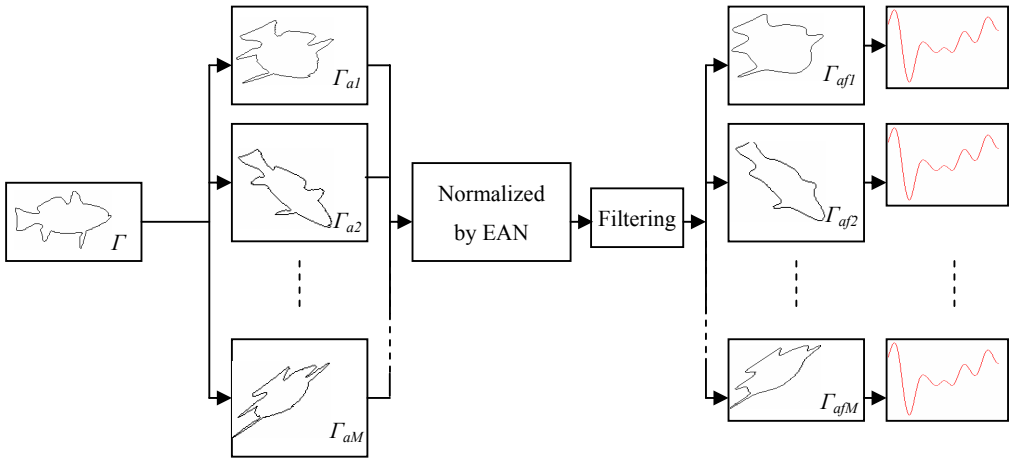

Fig.4. Demonstration of the theorem2

the curve $\Gamma_a(\mu)$ with a linear low-pass filter F whose impulse response is $g(\mu)$. In continuous form we have

$$\begin{aligned} x_{af}(\mu) &= x_a(\mu) * g(\mu) \\ &= [ax(\mu) + by(\mu)] * g(\mu) \\ &= ax(\mu) * g(\mu) + by(\mu) * g(\mu) \\ &= ax_f(\mu) + by_f(\mu) \end{aligned} \quad (4.5)$$

Where * denotes convolution. Likewise,

$$y_{af}(\mu) = cx_f(\mu) + dy_f(\mu) \quad (4.6)$$

Compare Eqs.4.5, 4.6 and Eqs.4.3, 4.4, it is clear that point $(x_{af}(\mu), y_{af}(\mu))$ is also the point $(x_f(\mu), y_f(\mu))$ transformed by the affine transform A. So the planar curve Γ_{af} is same as the planar curve Γ_{fa}.

The theorem1 indicates that after exchanging computation order between affine transform and filtering, there is no change in the result.

THEOREM2:

For any affine transform of a closed contour, using EAN to set the parameters produces planar curve $\Gamma_a(x_a(t), y_a(t))$. If area $s_p(t)$ is the area of an enclosed sector whose vertices are a pair of successive points and the centroid of the contour and if $\Gamma_{af}(x_{af}(t), y_{af}(t))$ indicates that Γ_a is filtered by a low-pass filter F, then the changes in enclosed areas $s_p(t)$ on the Γ_{af} are linear with affine mapping. See Fig.4.

PROOF:

In section 3, we know the enclosed area $s_p(t)$of the triangle on the contour filtered whose vertices are $(x_{af}(t), y_{af}(t))$, $(x_{af}(t+1), y_{af}(t+1))$ and the centroid G is

$$s_p(t) = \frac{1}{2} abs[x_{af}(t) y_{af}(t+1) - x_{af}(t+1) y_{af}(t)] \quad (4.7)$$

In the following, we will show that $s_p(t)$is absolutely affine invariant to affine transforms. Due to the THEOREM1,

$$x_{af}(t) = ax_f(t) + by_f(t) \quad (4.8)$$

$$y_{af}(t) = cx_f(t) + dy_f(t) \quad (4.9)$$

and

$$x_{af}(t+1) = ax_f(t+1) + by_f(t+1) \quad (4.10)$$

$$y_{af}(t+1) = cx_f(t+1) + dy_f(t+1) \quad (4.11)$$

Therefore from Eq.4.7

$$\begin{aligned} s_p(t) &= \frac{1}{2} abs\{ [ax_f(t) + by_f(t)][cx_f(t+1) + dy_f(t+1)] \\ &\quad - [ax_f(t+1) + by_f(t+1)][cx_f(t) + dy_f(t)]\} \\ &= \frac{1}{2} abs[adx_f(t) y_f(t+1) + bcx_f(t+1) y_f(t) \\ &\quad - adx_f(t+1) y_f(t) - bcy_f(t+1) x_f(t)] \\ &= \frac{1}{2} abs(ad - bc) \cdot abs[x_f(t) y_f(t+1) - x_f(t+1) y_f(t)] \end{aligned} \quad (4.12)$$

Observing the Eq.4.12, $s_p(t)$ is just linearly proportional by a scale factor $abs(ad-bc)$. Accordingly, we have proved that enclosed areas $s_p(t)$ are linear with affine mapping.

DEDUCTION:

The proportion $v'(t)$ of the closed areas $s_p(t)$ with the total area S of the filtered contour is preserved under general affine transforms .

PROOF:

According to Eq.4.12, the total area S of the filtered contour is:

$$S = \frac{1}{2} abs(ad - bc) \cdot \sum_{t=0}^{N-1} abs[x_f(t) y_f(t+1) - x_f(t+1) y_f(t)] \quad (4.13)$$

So

$$\begin{aligned} v'(t) &= s_p(t) / S \\ &= abs[x_f(t) y_f(t+1) - x_f(t+1) y_f(t)] \\ &\quad / \sum_{t=0}^{N-1} abs[x_f(t) y_f(t+1) - x_f(t+1) y_f(t)] \end{aligned} \quad (4.14)$$

Observe the Eq.4.14, $v'(t)$ doesn't relate with the affine parameters a, b, c and d . Therefore $v'(t)$ is preserved under general affine transforms.

In addition, we can deduct major property of $v'(t)$: the integration of $v(t) = [v'(t) - 1/N]$ equal to zero.

PROOF:

$$\sum_{t=0}^{N-1} v(t) = \sum_{t=0}^{N-1} [v'(t) - \frac{1}{N}] = \sum_{t=0}^{N-1} \frac{s_p(t)}{S} - \sum_{t=0}^{N-1} \frac{1}{N} = \frac{S}{S} - \frac{N}{N} = 0$$

We refer to vector $v(t)$ as the normalized part area vector (NPAV). As theorem2 and its deduction show, in all cases, even those with severe deformations, the function $s_p(t)$ is also preserved, only the amplitude changes under general affine transforms; the NPAV $v(t)$ has an affine-invariant feature.

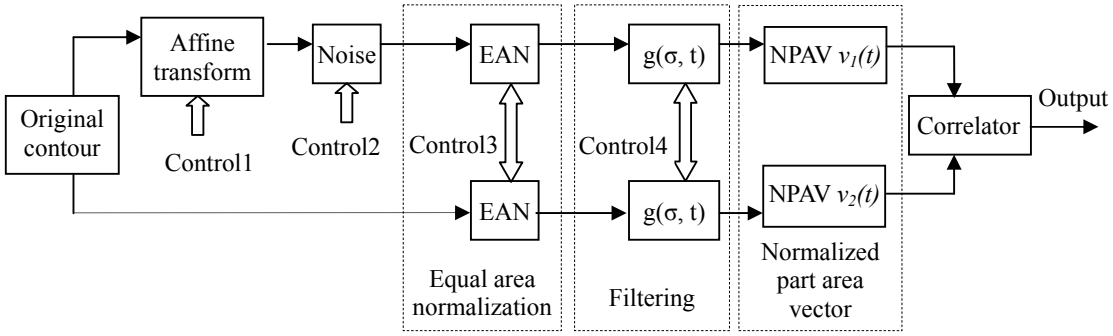

Fig.5. The framework of experiments

Ⅴ. EXPERIMENTAL RESULTS AND MULTISCALE NPAV

In experimental results, we will observe NPAV behavior in relation to affine transforms, EAN parameterization, filtering and noise. We experiment on the MPEG-7 CE-shape-1 database containing 1400 shape images. The framework of these experiments can be seen in Fig.5. Here, the low-pass filter is a Gaussian filter with a scale parameter σ. The evaluation output is the maximum linear correlation coefficient between the NSAV of the upper pathway after affine transforms, noise, EAN parameterization and filtering and the NSAV of the lower pathway with the original contour.

First, we evaluate the effect of affine transforms on NSAV. Let the number of normalized points be 512, the position of the starting point be the same as the original contour and σ=10. According to subsection Ⅱ.B, if the range of uniform scaling transforms and shearing transforms changes from 0.1 to 10 and the respective rotation angles are 60°, 120°, 180°, 240° and 300°, then all the linear correlation coefficients on NSAV have values above 97%.

We then assess the effect of equal area normalization (EAN) on NSAV. This experiment includes two aspects: on one hand the relation between NSAV and the number of points normalized by EAN and on the other hand the relation between NSAV and the position of the starting points on a contour. The results show that for a number of points on a contour normalized to 64, 128 and 256 , and simultaneously with a starting point position displaced to 12.5%, 25%, 37.5% and 50% of the index points along the contour, all the linear correlation coefficient values stay above 97%.

Finally, we study the effect of noise on NSAV. When we resample the edges of an object, the original shapes are affected by noise and impairments, generating fluctuations on the boundary. The general method for noise simulation on a contour is to shift the x, y coordinates of the points on a contour independently. In this way, the order of certain points on the contour becomes confused (cf. Fig.6(a)). However, in practice, such distortion cannot be present. In order to simulate the real effect of noise on an object, the displacement direction of each point affected by noise is controlled so that it is only vertical to the tangent of the point. Fig.6(b) shows the effect of noise simulated with the proposed method i.e. there is a significant decrease in self-intersections.

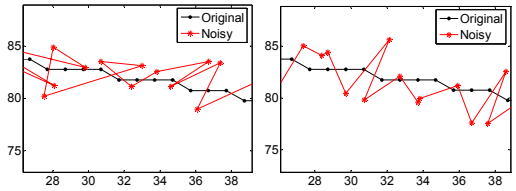

(a) (b)

Fig.6. Two effects of adding simulated noise. (a) is the effect of the general method of simulation. (b) is the effect of the proposed method

If its amplitude is controlled by a uniform random value, suppose the amplitude range is *[-r, r]*, and the average distance between all the points on the contour and its centroid is *D*, we define the signal-to-noise ratio (*SNR*) as follows:

$$\mathrm{SNR} = 20\lg\frac{2D}{r}(\mathrm{dB})$$

We performed the experiments in such a way that the test contours were contaminated by random uniform noise ranging from high to low *SNRs* (cf. Fig.7(a)-(d)).

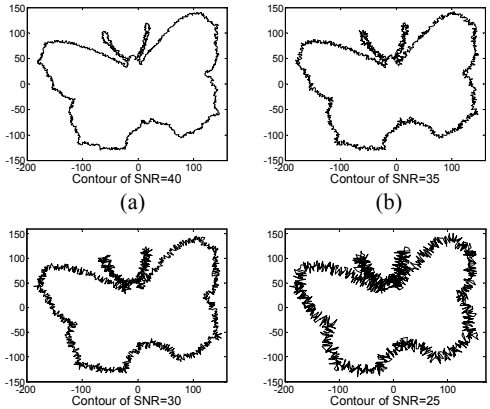

(a) (b) (c) (d)

Fig.7. Demonstration of a contour contaminated by various SNRs.

Table Ⅰ. The average correlation coefficient of different SNR

SNR	Correlation coefficient
40dB	0.96366
35dB	0.96298
30dB	0.94907
25dB	0.89765

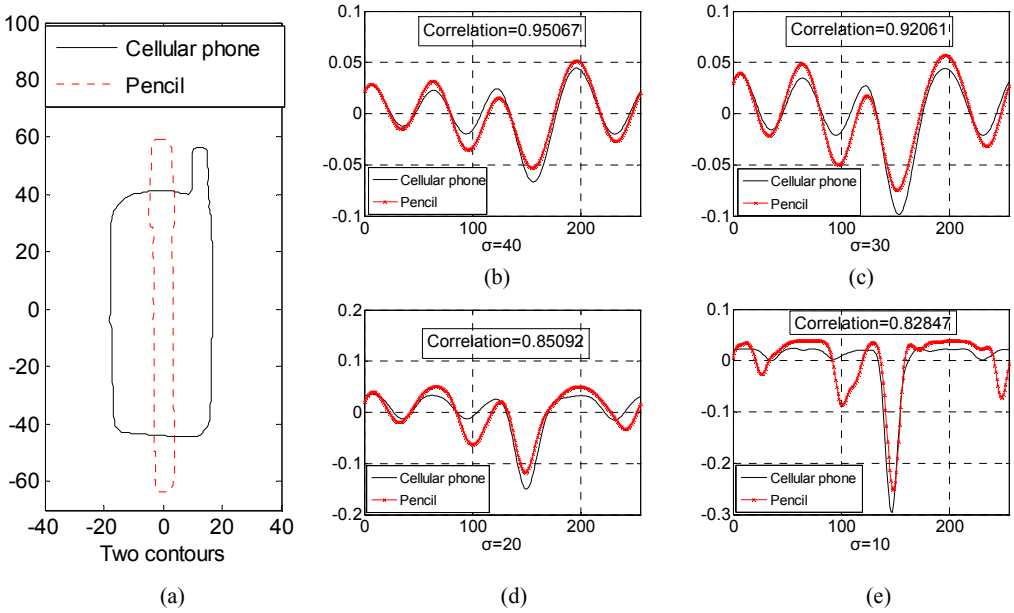

Fig.8. NPAV and the scale. (a) is two original contours. (b)-(e) are their NPAVs with different scale.

Table Ⅰ shows the average correlation coefficient of all the NSAVs of shapes in the database with different *SNRs*. Correlation between NSAVs remains at an adequate level to allow efficient pattern recognition.

By analysing the results of experiments, we notice that NPAV is quite robust with respect to scale, orientation changes of objects, shearing, the position of starting point and the noise. Therefore, NPAV can be used to characterize a pattern for recognition purpose. In the following, we propose the object recognition scheme based on multiscale technology.

Under the high scale, it's possible that some of objects different have the similar NPAV. However the NPAVs of these objects have probably different feature under low scale. Fig.8 shows an example, the two objects in (a) are normalized by EAN to 256 points. Fig.8 (b)-(e) are their NPAVs under the scale $\sigma = 40$, $\sigma = 30$, $\sigma = 20$ and $\sigma = 10$ respectively. As can be seen in figures, the higher scale is, the more similar they are. On the contrary, the lower scale is, the more different they are. So we can present a shape with different scale: high-scale NPAV can be used to eliminate dissimilar shapes and low-scale images can discriminate between similar shapes.

In addition, as the NPAV expresses a contour with all the points normalized by EAN, it is rather redundant. To decrease the redundancy, we apply the wavelet algorithm to compress the NPAV. We have noticed that the higher the value of σ, the less high frequency remains in the NPAV, on the contrary, the lower the value of σ, the more high frequency remains in it. So we can use the high compress ratio to NPAV with higher σ, and low compress ratio to that with lower σ. In this way, a high computationally efficient object recognition scheme can be designed.

Ⅵ. CONCLUSION

In this paper, a new method of extracting invariants of an image under affine transform is described. Our representation is based on the association of the two parameters the affine arc length and enclosed area, viz. we normalize a contour to invariant length by the affine enclosed area. We then prove two theorems and a deduction. They reveal that for a filtered contour, the part area is linear under affine transforms. We further define an affine-invariance vector: normalized part area vector (NPAV). A number of experiments on the MPEG-7 database demonstrate that NPAV is quite robust with respect to affine transforms and noise, even in the presence of severe noise. In addition, we propose a method to simulate the noise contaminating the test shapes and define the signal-to-noise ratio for a shape. Finally, a shape recognition scheme is briefly presented.

Future directions of the research include doing more extensive tests to assess retrieval results by multiscale NPAV, ameliorating the retrieval performance of the NPAN under part of the shape occluded.

REFERENCES

[1] Erdem Bala, A. Enis Cetin, Computationally Efficient Wavelet Affine Invariant Functions for Shape Recognition, IEEE Trans. Pattern Analysis and Machine Intelligence, vol.26, no.8, pp.1095-1099, 2004.

[2] K. Arbter, W.E. Snyder, H. Burkhardt, G. Hirzinger, Applications of affine-invariant Fourier descriptors to recognition of 3-D objects, IEEE Trans. Pattern Analysis and Machine Intelligence, vol.12, no.7, pp.640-646, 1990.

[3] Mokhtarian, F. & Abbasi, S., Shape similarity retrieval under affine transform. Pattern Recognition, vol.35, no.1, pp.31-41, 2002.

[4] D. Cyganski, R.F. Vaz, A linear signal decomposition approach to affine invariant contour identification, Proceedings of SPIE-Intelligent Robots and Computer Vision X: Algorithms and Techniques, vol.1607, pp.98-109, 1991.

[5] A. Zhao, J. Chen, Affine curve moment invariants for shape recognition, Pattern Recognition, vol.30, no.6, pp.895-901, 1997.

[6] Quang Minh Tieng, Wageeh W. Boles, Wavelet-Based Affine Invariant Representation: A Tool for Recognizing Planar Objects in 3D Space, IEEE Trans. Pattern Analysis and Machine Intelligence, vol.19, no.8, pp.846-857, 1997.